SCIENTIFIC REPORTS

Suppression of Structural Phase Transition in VO$_2$ by Epitaxial Strain in Vicinity of Metal-insulator Transition

Mengmeng Yang[1,2], Yuanjun Yang[1,2,3], Bin Hong[1,2], Liangxin Wang[1], Kai Hu[1], Yongqi Dong[1,2], Han Xu[4], Haoliang Huang[3], Jiangtao Zhao[1], Haiping Chen[1], Li Song[1], Huanxin Ju[1], Junfa Zhu[1], Jun Bao[1], Xiaoguang Li[4], Yueliang Gu[5], Tieying Yang[5], Xingyu Gao[5], Zhenlin Luo[1,2] & Chen Gao[1,2,3]

Mechanism of metal-insulator transition (MIT) in strained VO$_2$ thin films is very complicated and incompletely understood despite three scenarios with potential explanations including electronic correlation (Mott mechanism), structural transformation (Peierls theory) and collaborative Mott-Peierls transition. Herein, we have decoupled coactions of structural and electronic phase transitions across the MIT by implementing epitaxial strain on 13-nm-thick (001)-VO$_2$ films in comparison to thicker films. The structural evolution during MIT characterized by temperature-dependent synchrotron radiation high-resolution X-ray diffraction reciprocal space mapping and Raman spectroscopy suggested that the structural phase transition in the temperature range of vicinity of the MIT is suppressed by epitaxial strain. Furthermore, temperature-dependent Ultraviolet Photoelectron Spectroscopy (UPS) revealed the changes in electron occupancy near the Fermi energy E_F of V 3d orbital, implying that the electronic transition triggers the MIT in the strained films. Thus the MIT in the bi-axially strained VO$_2$ thin films should be only driven by electronic transition without assistance of structural phase transition. Density functional theoretical calculations further confirmed that the tetragonal phase across the MIT can be both in insulating and metallic states in the strained (001)-VO$_2$/TiO$_2$ thin films. This work offers a better understanding of the mechanism of MIT in the strained VO$_2$ films.

Vanadium dioxide (VO$_2$) is an archetypal correlated material discovered by Morin with excellent metal-insulator transition (MIT) characteristics at the critical temperature (~68 °C in bulk state)[1]. Due to the optical transmittance changes at the infrared[2] and THz regions[3,4] and huge resistance jump[5], VO$_2$ has become a widely-studied material in fundamental studies and for industrial applications such as metamaterials[6–8], smart windows[9], supercapacitors[10], etc. Generally, the MIT of bulk VO$_2$ or nanobeam-like counterparts always accompanies a structural phase transition from a low temperature monoclinic phase to a high temperature tetragonal phase[11–13]. However, this hypothesis does not always hold.

Indeed, there is still a significant debate over whether the mechanism of MIT in VO$_2$ is a Mott transition[14,15], Peierls transition[16,17], or a combination of the two[18,19]. As early as 1975, Zylbersztejn and Mott showed that the mechanism of MIT in VO$_2$ was not the simple Mott-Hubbard transition induced only by electron-electron interactions[20]. In 2004, Cavalleri et al. found evidence for a structure-driven MIT in VO$_2$ by ultrafast spectroscopy and declared that the mechanism of MIT was not the Mott-Hubbard transition[11]. However, Kim et al. observed

[1]National Synchrotron Radiation Laboratory, University of Science and Technology of China, Hefei, Anhui 230026, China. [2]Collaborative Innovation Center of Chemistry for Energy Materials, University of Science and Technology of China, Hefei, Anhui 230026, China. [3]CAS Key Laboratory of Materials for Energy Conversion, Department of Materials Science and Engineering, University of Science and Technology of China, Hefei, Anhui 230026, China. [4]Department of Physics, University of Science and Technology of China, Hefei, Anhui 230026, China. [5]Shanghai Synchrotron Radiation Facility, Shanghai Institute of Applied Physics, Chinese Academy of Sciences, Shanghai 201204, China. Correspondence and requests for materials should be addressed to Y.Y. (email: yangyuanjun@ustc.edu.cn) or Z.L. (email: zlluo@ustc.edu.cn) or C.G. (email: cgao@ustc.edu.cn)
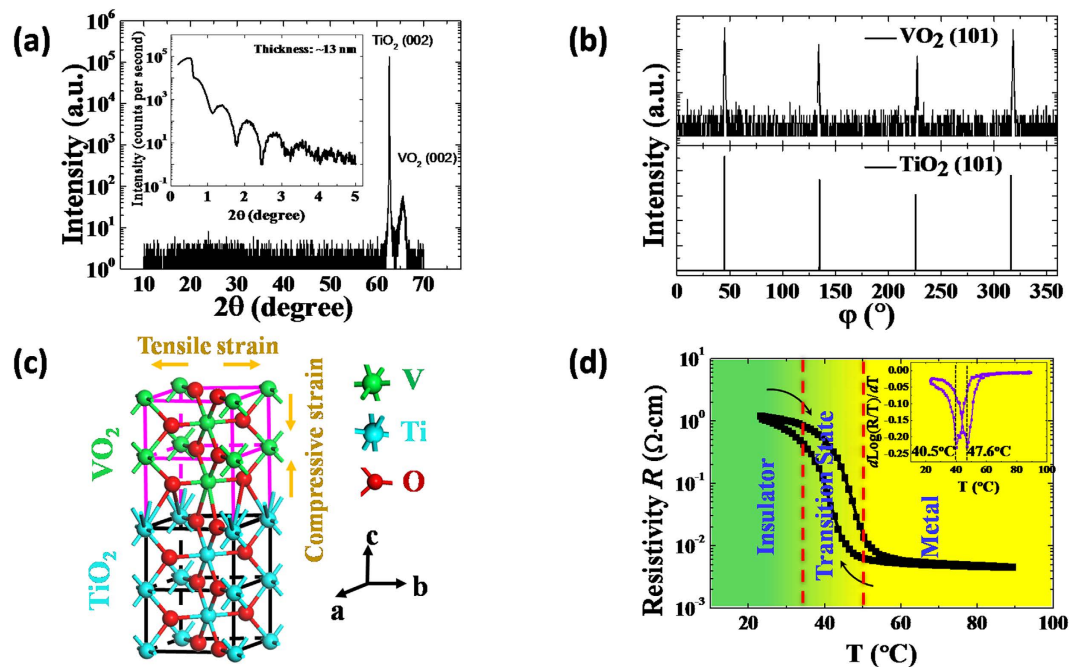
Figure 1. (a) XRD θ–2θ patterns of ultrathin VO_2/TiO_2 film, inset: XRR curve. (b) The XRD φ scans of the (101) peaks of VO_2 film and TiO_2 substrate at room temperature. (c) The schematic crystal structures of ultrathin VO_2 film on TiO_2 substrate. (d) The R-T curve of the ultrathin VO_2/TiO_2 film and corresponding differential curve.

that the tetragonal metallic phase did not occur simultaneously with MIT by the ultrafast pump-probe technology—they ascribed the MIT to the Mott mechanism illustrated by photo-assisted hole excitation[21]. Thus, the mechanism of MIT remains controversial—some researchers[22,23] believe that the MIT is induced by the broken symmetry of lattice, namely, the Peierls transition. Concurrently, there are many others who believe that the MIT in VO_2 is a Mott transition[14,24].

On the other hand, epitaxial strain due to lattice mismatch between thin film VO_2 and substrates has revealed a different picture of the MIT[22]. A tetragonal phase was identified by transmission electron microscopy in the ultrathin VO_2 layers just adjacent to the TiO_2 substrate in Zou's work[25], and X-ray diffraction reciprocal space mapping (XRD-RSM) suggested that there is no monoclinic phase in ultrathin VO_2 films at room temperature[25]. Furthermore, our recent findings demonstrated an anomalous tetragonal-like to tetragonal structural phase transition but not a conventional monoclinic to tetragonal phase transition in 300-nm-thick VO_2/TiO_2 films (not shown here). In addition, Jiwei Lu *et al.* proposed a Mott-like phase transition in VO_2 thin films induced by a large bi-axial epitaxial strain based on Raman spectroscopy data[26]. Laverock *et al.* observed a crossover from a Mott-Peierls-like transition to a Mott-like transition by large out-of-plane tensile in strained VO_2 thin films through various spectroscopic techniques[27].

All of these observations have demonstrated that the structural evolution in the strained VO_2 thin films was complicated by epitaxial strain, which could lead a misunderstanding of the role of structural phase transition in the MIT. Therefore, epitaxial strain plays a very important part in not only modulating the MIT behaviors but also understanding the underlying mechanism of MIT in the strained VO_2 thin films. To date, the mechanism of MIT in strained VO_2 thin films has not been completely addressed. Moreover, the low-temperature phase in thin film VO_2 under substrate clamping has not yet been fully understood and identified—this is very important for unveiling the MIT mechanism in ultrathin VO_2 epitaxial films.

In this study, we investigated the evolutions of crystal structure and electronic states in the ultrathin VO_2 films grown on (001)-oriented TiO_2 substrates via temperature-dependent XRD-RSM, Raman spectroscopy and Ultraviolet Photoelectron Spectroscopy (UPS). We found that the absence of the structural phase transition across the MIT—and thus the electronic transition—may solely trigger the MIT. Moreover, the insulating tetragonal VO_2 at room temperature is stabilized by epitaxial strain, which is further confirmed by density functional theory (DFT) calculations. To the best of our knowledge, this is a systematic report to investigate the structural and electronic transition of VO_2 films grown on (001)-oriented TiO_2 substrates combining XRD-RSM, Raman spectroscopy, UPS tools and theoretical methods—the findings also have important implications for researchers in the field of optics and electronics.

Results and Discussion

Crystal structure evolution across MIT. To evaluate the quality of the VO_2 thin film, the XRD θ–2θ patterns of (001)-VO_2/TiO_2 thin film were acquired (Fig. 1a). As shown in Fig. 1a, only the (002) peaks of the VO_2 thin film and TiO_2 substrate appear, which suggests that the VO_2 thin film is highly oriented along the

out-of-plane direction of the TiO$_2$ substrate. According to the small angle X-ray reflection (XRR) in the inset of Fig. 1a, there are clear thickness-interference fringes suggesting that the surface of the VO$_2$ thin film is smooth. Both atomic force microscopy and polarized optical microscopy confirmed the smooth surface (root mean square: ~0.4 nm) and uniformity of VO$_2$ thin films (not shown here). We thus can calculate the thickness (h) with the formula[28]:

$$h = \frac{(m-n)\lambda}{2(\sin\theta_m - \sin\theta_n)} \tag{1}$$

where m and n are the orders of interference, and θ_m and θ_n are the corresponding diffraction angles, respectively. The VO$_2$ thickness is calculated to be ~13 nm, which is thin enough to maintain the epitaxial strain between the VO$_2$ thin film and TiO$_2$ substrate well below the critical thickness (~26.5 nm)[26,29].

From the XRD φ scans of (101) peaks of TiO$_2$ substrate at room temperature in Fig. 1b, there are four peaks, each separated by 90°. This originates from the nature of four-fold symmetry of the TiO$_2$ substrate. For the VO$_2$ thin film, the (101) peaks (defined by tetragonal unit cell) from the φ scans have located the same azimuthal angles as those in the TiO$_2$ substrate (Fig. 1b). Therefore, the 13-nm VO$_2$ thin film grows epitaxially on the tetragonal TiO$_2$ substrate and has a similar symmetry as the TiO$_2$ substrate at room temperature. This implies the four-fold symmetry of the VO$_2$ thin film. And thus the epitaxial relationship between the VO$_2$ thin film and TiO$_2$ substrate is $[001]_{VO_2}$ // $[001]_{TiO_2}$ along the out-of-plane direction, and $[010]_{VO_2}$ // $[010]_{TiO_2}$ and $[100]_{VO_2}$ // $[100]_{TiO_2}$ along the in-plane direction. This relationship is shown schematically at Fig. 1c. We can imagine that the ultrathin VO$_2$ film probably suffers tensile strain along the in-plane direction because the in-plane lattice constant a of TiO$_2$ substrate is larger than that of bulk VO$_2$. The compressive strain should be correspondingly developed along the out-of-plane direction with assumption of conservation of volume of the VO$_2$. The strain states in the (001)-VO$_2$ epitaxial film are shown in Fig. 1c.

Importantly, the 13-nm (001)-VO$_2$ epitaxial film is in the tetragonal phase at room temperature as shown by the above symmetry analysis of the diffraction peaks. The Raman data offers additional evidence regarding the low-temperature tetragonal phase in this VO$_2$ thin film, but this contradicts with the previous reports[30] in which the monoclinic phase (M1) of the 110 nm-thick VO$_2$ films were studied at room temperature. We conjecture that epitaxial strain should stabilize the tetragonal phase in the thinner (001)-VO$_2$/TiO$_2$ film versus the cases in the literature[27,31] at room temperature. However, the relaxation of the epitaxial strain in the thicker VO$_2$ thin film resulted in the formation of the observed M1 phase at room temperature (see Raman spectra below).

Figure 1d shows the R-T curve of the ultrathin (001)-VO$_2$/TiO$_2$ film and corresponding differential curve during the temperature cycling from room temperature to 90 °C and backward. The resistivity shows an abrupt jump at the transition temperature (T$_{MIT}$) of ~47.6 °C (Fig. 1d inset), which is lower than that of the bulk counterpart. Moreover, the change of resistivity across the MIT is up to three orders of magnitude, which is comparable to previous reports[25]. These could be closely related to the modulation of the electronic structures by epitaxial strain[32-34]. It is mentionable that the MIT in the present work is a bit higher than the previous reports (~36 °C)[26] with the similar film thickness. First, the Ti interdiffusion partially accounts for the increasing the MIT in the VO$_2$/TiO$_2$ epitaxial films. Y. Muraoka et al. found that the high growth temperature can induce the Ti diffusion to the VO$_2$ thin films and dramatically increase the MIT from 28 °C to 67 °C in the 12-nm (001)-VO$_2$/TiO$_2$ films grown by pulse laser deposition technique[35]. And the interdiffusion region was observed to be restricted to 1.2 nm at the interface between the VO$_2$ film and TiO$_2$ substrate by Quackenbush et al.[36]. Second, the oxygen pressure for the VO$_2$ film growth may introduce non-stoichiometry and change the MIT obviously. Stuart S. P. Parkin et al.[37] found the MIT of the 10-nm (001)- VO$_2$/TiO$_2$ films was changed from 17 °C to 28 °C with increasing the growth oxygen pressure. Junhao Chu et al.[38] also observed a dramatic increasing of the MIT from 48 °C to 75 °C in the VO$_2$/Al$_2$O$_3$ epitaxial films. The possible reason for this may be ascribed to the balance of the doping level and acceptor level in the forbidden gap produced by oxygen vacancy and vanadium vacancy in different growth oxygen pressure, respectively[38,39]. Third, the MIT becomes higher with the larger lattice constant c as reported in refs 26,35,37. The long V^{4+}–V^{4+} distance relieves the direct overlapping of d orbitals, which decreases the width of the d band and increases the MIT in the tetragonal structure of the (001)-VO$_2$/TiO$_2$ films[35]. Therefore, the structural studies and electrical measurements both highlight the excellent quality of the sample and these samples demonstrate the apparent MIT in the (001)-VO$_2$/TiO$_2$ epitaxial films, which is as similar as the metal-insulator transition behaviors in the previous studies[34-39].

To illustrate the correlations between the mechanism of MIT and structural phase transition in the strained (001)-VO$_2$/TiO$_2$ epitaxial film, the structure evolution across MIT was studied by in situ temperature-dependent high resolution XRD with reciprocal space mapping (RSM) technique. The evolution of RSMs around (002) and (112) diffractions of VO$_2$/TiO$_2$ are presented in Fig. 2. There are two Bragg spots in each RSM—the lower one belongs to TiO$_2$ substrate and the upper one belongs to the VO$_2$ film. The RSMs were plotted in reciprocal lattice units (r.l.u.) of the TiO$_2$ substrate (1 r.l.u. = 2π/2.9592 Å^{-1}). The (002) and (112) peaks of the VO$_2$ film in the RSMs (Fig. 2) didn't move across all the entire heating and cooling process. This strongly indicates that there is no structural phase transition occurring during the MIT. In other words, this behaviour is not consistent with the previous reports in the refs.11–13, in which the electronic transition is always accompanied with a structural phase transition. However, Jiwei Lu et al.[26] recently reported a Mott-like phase transition in VO$_2$ films induced by a large epitaxial bi-axial strain using Raman spectroscopy. This suggests that the structural phase transition did not always appear during the MIT. Our findings in the strained (001)-VO$_2$/TiO$_2$ films agree well with the Lu's results. Moreover, this study offers direct evidence of a microscopic crystal structure for the suppression of structural phase transition by epitaxial strain. Therefore, we believe that MIT in this ultrathin (001)-VO$_2$/TiO$_2$ film may be driven solely by electronic transition.
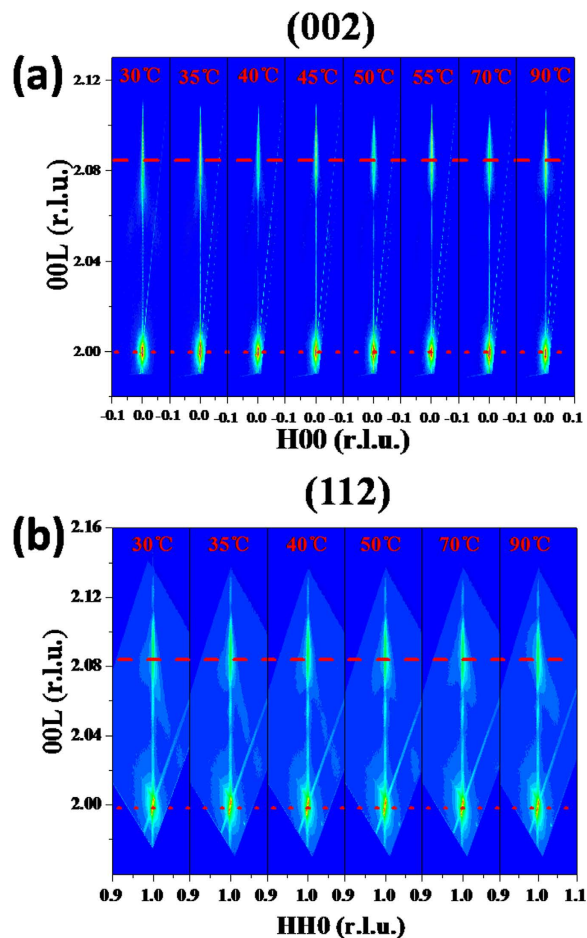
Figure 2. Temperature-dependent RSMs of (**a**) (002) and (**b**) (112) diffraction spots for ultrathin (001)-VO$_2$/TiO$_2$ thin film.The red dotted and dashed lines represent the positions of the TiO$_2$ substrate and VO$_2$ film, respectively.

From the RSMs of (002) and (112) peaks of the ultrathin (001)-VO$_2$/TiO$_2$ film, the lattice constants c and a allow calculation of strain:

$$strain = \frac{d_f - d_b}{d_b} \times 100\%$$

$$(2)$$

where d_f and d_b are the lattice constants of the VO$_2$ thin film and its bulk counterpart, respectively. The corresponding strains were calculated to be −0.58% along the out-of-plane direction and +0.86% along the in-plane direction without relaxation of the in-plane strain—this is consistent with the previous report[40]. Thus, the ultrathin (001)-VO$_2$/TiO$_2$ films suffer the bi-axial strains, suppressing the structural phase transition across the MIT.

To directly see the changes in the lattice constant across the MIT, we calculated the out-of-plane lattice constants based on the temperature-dependent RSMs in Fig. 2 and plotted them in Fig. 3. For comparison, we prepared a thicker (001)-VO$_2$/TiO$_2$ film (~60 nm) and the corresponding out-of-plane lattice constants c is shown in the upper part of Fig. 3. The thicker film presented an obvious abrupt jump in the lattice constant c, which clearly suggests a structural phase transition during MIT. Moreover, the lattice constant c is about 2.854 Å in the high-temperature tetragonal phase (above 65 °C), which is nearly as same as the bulk one (~2.8557 Å). Therefore, the epitaxial strain should be also relaxed along the in-plane directions in the thicker films. The temperature-dependent XRD θ–2θ fine scans to determine lattice constant c are shown in Supporting Information (Figs S1 and S2). However, the lattice constants c of the 13-nm-thick VO$_2$/TiO$_2$ epitaxial film were nearly constant regardless of calculation via the (002) or (112) diffraction spots. The slight increase in the lattice c may be due to the thermal expansion of the VO$_2$[36]. This result directly shows that there is no structural phase transition during MIT for the strained (001)-VO$_2$/TiO$_2$ epitaxial film.

Raman analysis for the microstructure across the MIT.   To further confirm the lack of structural phase transition in the ultrathin VO$_2$ thin film, Raman scattering spectroscopy was used to study the lattice vibrations of VO$_2$ across the MIT[41–46]. It is well known that the monoclinic and tetragonal phases of VO$_2$ thin films have the
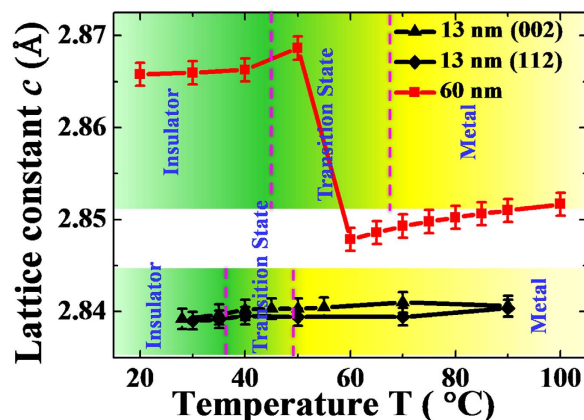
Figure 3. The lattice constant *c* as a function of temperature for 13-nm and 60-nm VO$_2$ films. The red square line represents the *c* of 60-nm VO$_2$ thin film. The triangle and diamond lines represent the *c* of the 13-nm VO$_2$ thin film calculated from (002) and (112) diffraction spots in the RSMs, respectively. The mixed regions of yellow and green shadows highlight the transition temperature ranges of the 13-nm and 60-nm films that were divided by dashed lines.
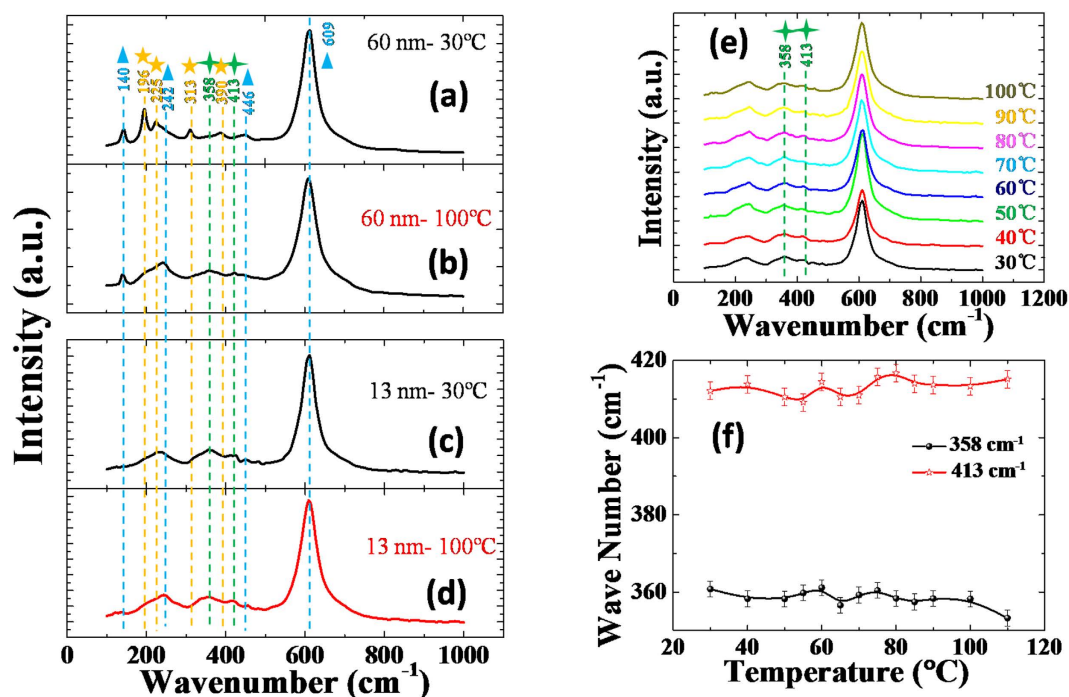
Figure 4. Raman spectrum of 60 nm (001)-VO$_2$/TiO$_2$ thin film at (**a**) 30 °C and (**b**) 100 °C of the 13-nm (001)-VO$_2$/TiO$_2$ thin film at (**c**) 30 °C and (**d**) 100 °C. The blue triangles, yellow stars, and green squares and corresponding dotted lines label the Raman peaks in the TiO$_2$ substrate, the monoclinic phase VO$_2$, and the tetragonal phase VO$_2$, respectively. (**e**) Temperature-dependent Raman spectroscopy of ultrathin (001)-VO$_2$/ TiO$_2$ thin film. (**f**) The Raman peaks belong to the tetragonal phase VO$_2$ and are a function of temperature.

distinctly different Raman features: the former displays several sharp Raman peaks, while the latter is characterized by a broadband peak[41]. Hence we performed temperature-dependent Raman spectroscopy measurements for both thick and thin VO$_2$ films as shown in Fig. 4.

The data in Fig. 4a shows the Raman spectrum of the 60 nm-thick VO$_2$/TiO$_2$ thin film at 30 °C with four sharp peaks at 196 cm^{-1}, 225 cm^{-1}, 313 cm^{-1}, and 390 cm^{-1}. These peaks are the representative A$_g$ vibration modes of the monoclinic VO$_2$[37–40]. However, these four characteristic Raman peaks disappears at 100 °C (Fig. 4b). This indicates that the 60-nm-thick VO$_2$/TiO$_2$ film undergoes a structural phase transition from low-temperature monoclinic phase to high temperature tetragonal phase during the MIT. On the other hand, the above four Raman peaks belonging to monoclinic phase VO$_2$ do not exist in the Raman spectrum of the 13-nm-thick VO$_2$ thin film at 30 °C or 100 °C (see Fig. 4c,d). Hence, there are no monoclinic components of the VO$_2$ in the
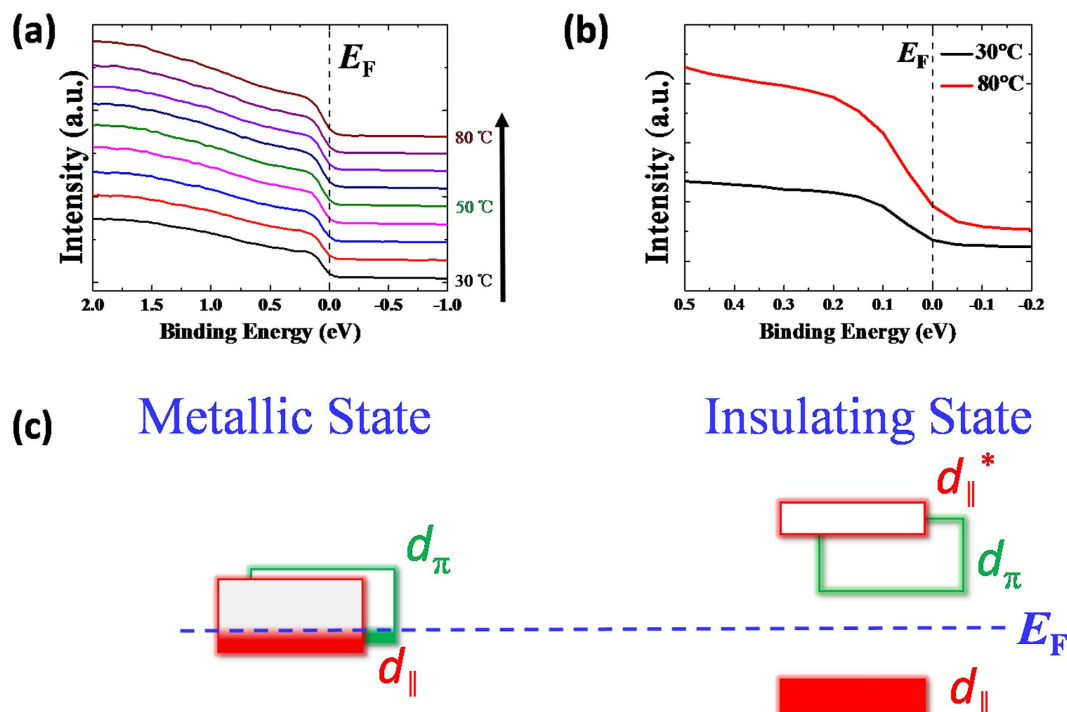
Figure 5. (**a**) The V 3d orbital electronic states near Fermi energy E_F with varying temperature from 30 to 80 °C. (**b**) The selected and expanded V 3d electronic states at 30 °C and 80 °C. (**c**) The band occupancies of V 3d electrons near Fermi energy E_F both at insulating and metallic states.

strained (001)-VO$_2$/TiO$_2$ thin film at low temperature or high temperature. Furthermore, the Raman spectrum of the ultrathin VO$_2$ thin film at 30 °C and 100 °C both have the two broad Raman peaks at about 358 cm^{-1} and 413 cm^{-1}, which resembles the Raman spectrum of the thicker VO$_2$ thin film at 100 °C in Fig. 4b, where the VO$_2$ is exactly right in the tetragonal symmetry. Therefore, it is suspected that the above two broad Raman peaks belong to the tetragonal phase VO$_2$ based on the conclusion that 60-nm-thick VO$_2$ films experience a MIT from low temperature monoclinic phase to high temperature tetragonal phase. Interestingly, the two peaks did not move across the MIT for the case of the ultrathin (001)-VO$_2$/TiO$_2$ thin film in Fig. 4c,d, suggesting that the tetragonal phase in the ultrathin (001)-VO$_2$/TiO$_2$ film is stabilized by epitaxial strain regardless of low or high temperature.

In order to clearly show the microstructure evolution of the ultrathin (001)-VO$_2$/TiO$_2$ film across the MIT, we preformed the fine temperature-dependent Raman spectroscopy measurements as shown in Fig. 4e (Supporting Information Fig. S3). There are no sharp Raman peaks belonging to the monoclinic phase during the MIT indicating the absence of monoclinic phase in the strained (001)-VO$_2$ thin films. In addition to the Raman peaks of the TiO$_2$ substrate (140 cm^{-1}, 242 cm^{-1}, 446 cm^{-1}, and 609 cm^{-1}; blue triangles in Fig. 4d, Supporting Information Fig. S4)[45], there are only two Raman peaks (358 cm^{-1} and 413 cm^{-1})—these belong to the tetragonal phase VO$_2$. For clarity, we plotted the two peak positions as a function of temperature in Fig. 4f. The two peaks showed no clear shift during MIT, implying that there is no structural phase transition across the MIT for the strained (001)-VO$_2$/TiO$_2$ thin films.

Based on these XRD studies and Raman spectroscopy analysis, we concluded that the tetragonal phase is stabilized by epitaxial strain—there is no monoclinic VO$_2$ at room temperature, but instead of the tetragonal phase. Consequently, the structural phase transition is not a necessary condition for the MIT in strained (001)-VO$_2$/TiO$_2$ thin films.

Studies on electron occupancy near Fermi level by temperature-dependent UPS. We next mainly studied the electronic transition of the ultrathin (001)-VO$_2$/TiO$_2$ thin film across the MIT by temperature-dependent UPS[47–52] because the structural phase transition was suppressed in the vicinity of the MIT temperature in such strained films. Figure 5a shows the UPS of ultrathin (001)-VO$_2$/TiO$_2$ thin film from 30 °C to 80 °C to track the change of the V 3d electronic states from low temperature insulating state to high temperature metallic states. For clarity, the UPS spectrum at 30 °C and 80 °C were selected to zoom in near the Fermi level (Fig. 5b). At 30 °C, there are fewer electrons occupying the Fermi Energy E_F, and the occupancy rises as a function of temperature up to 80 °C (Supporting Information Fig. S5). On the basis of crystal-field theory[53,54], the chemical bonds are associated with the p-d hybridization between the O 2p and V 3d orbitals, and thus formed the d$_\parallel$ and d$_\pi$ orbitals (Fig. 5c). During the MIT, the lowering of the crystal symmetry from rutile to monoclinic lifts the orbital degeneracy. The formation of the V-V dimers along the rutile c axis splits the nonbonding d$_\parallel$ states into occupied and unoccupied d$_\parallel$* states. Meanwhile the zigzagging of the V-V pairs shifts the d$_\pi$ state to higher energies, which opens the band gap in the insulating phase[54]. The occupancy in the metallic state is higher than
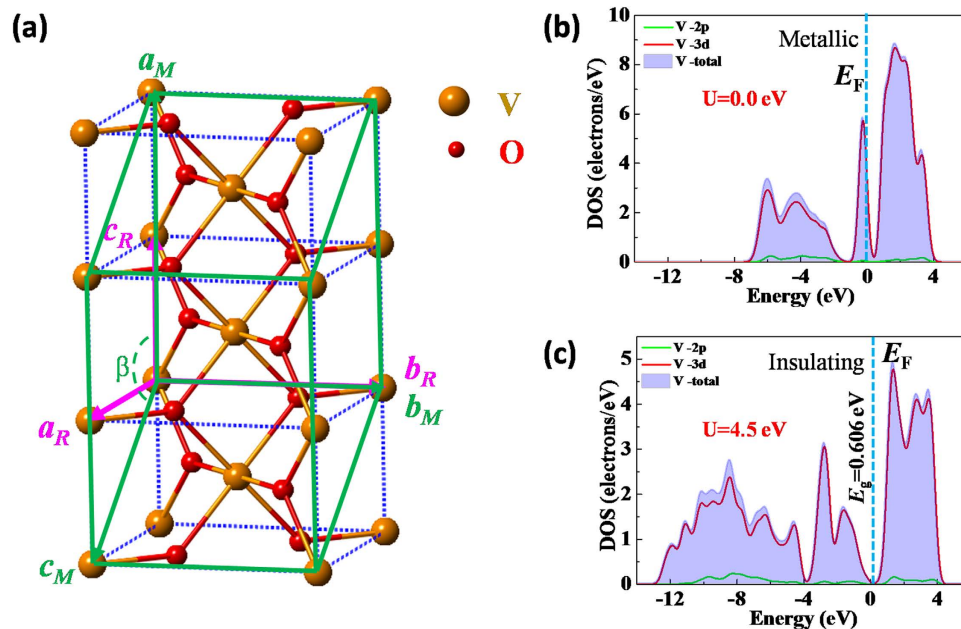
Figure 6. (**a**) The chosen super cell of VO_2 for calculation. The green lines show the super cell of VO_2 for DFT calculations. The calculated PDOS spectra of V with (**b**) $U = 0.0\,eV$ and (**c**) $U = 4.5\,eV$.

that in insulating state near the Fermi energy E_F. This demonstrates that the electronic transition occurred during MIT for ultrathin VO_2 films.

DFT Calculations. We used density functional theory (DFT+U) calculations to verify the suppression of structural phase transition and modulation of the electron occupancy. The DFT+U method has well described the phase transition in VO_2 system[55,56], where U is the Hubbard electron−electron correlation parameter. Figure 6a shows the chosen super cell of VO_2 for DFT calculations with different U. The experimental lattice constants under strained condition from our XRD results were used for calculations. For the tetragonal unit cell, the lattice constants are $a_T = b_T = 4.584\,Å$, $c = 2.831\,Å$, $\alpha_T = \beta_T = \gamma_T = 90°$, and the lattice constants of super cell are $a_S = 5.661\,Å$, $b_S = 4.584\,Å$, $c_S = 5.387\,Å$, $\alpha_S = \gamma_S = 90°$, $\beta_S = 121.7°$, which are transformed from the tetragonal unit cell with the formula:

$$\begin{bmatrix} a_s \\ b_s \\ c_s \end{bmatrix} = \begin{bmatrix} 0 & 0 & 2 \\ 0 & 1 & 0 \\ 1 & 0 & -1 \end{bmatrix} \begin{bmatrix} a_T \\ b_T \\ c_T \end{bmatrix}$$

(3)

The calculated projected density of states (PDOS) for the metallic state is shown in Fig. 6(b) with Hubbard electron-electron correlation energy $U = 0.0\,eV$. The PDOS for the insulating state with the chosen Hubbard electron-electron correlation energy $U = 4.5\,eV$ based on previous studies[55,57,58] is plotted in Fig. 6c. (Please see the details of DFT calculations in Supporting Information Fig. S6)[55,59]. It is well understood that the high-temperature tetragonal phase of VO_2 was metallic due to the electron occupancy at Fermi energy E_F[57]—this is seen in Fig. 6b. However, the VO_2 was an insulating state at low temperature because of the appearance of band gap E_g near the Fermi energy E_F[57], which may be induced by the electron-electron correlations. It is noted that the crystal structure used in calculations is locked whatever for the $U = 0.0\,eV$ and $U = 4.5\,eV$. Therefore, we concluded that the ultrathin strained VO_2 film changed from insulating to metallic states without the assistance of structural phase transition. The tetragonal insulating phase can survive with the help of epitaxial strain even at room temperature[58]. The electronic transition should be the only driving force for the MIT in this strained (001)-VO_2/TiO_2 epitaxial films.

Thickness effect on the structural phase transition of strained VO_2 films. Based on the above results and discussion, we can conclude that the structural phase transition during MIT for the ultrathin and nanoscale-strained (001)-VO_2/TiO_2 film is suppressed. The electronic transition and structural phase transition is separated in the highly strained (001)-VO_2/TiO_2 epitaxial films[26]. The electronic transition is the unique driving force that triggers the MIT. Therefore, the MIT of ultrathin VO_2 films should be a pure Mott transition. This behavior can be ascribed to the interfacial epitaxial strain between the VO_2 thin film and the TiO_2 substrate[25–27].

In terms of hetero-epitaxial systems[29], the (001) oriented VO_2 film is very easy to grow epitaxially along the lattice of tetragonal (001)-TiO_2 substrate because of the tiny in-plane lattice mismatch ($\sim$−0.86%) between them[29]. Thus, the VO_2 film is stabilized in the tetragonal structure at the initial interface under substrate constraint as described in the 13-nm-thick (001)-VO_2/TiO_2 epitaxial films. We also performed structural studies on the 24-nm-thick case. The results also evidenced the absence of the structural phase transition across the MIT

(see Supporting Information Figs S7 and S8). Therefore, the entire ultrathin VO$_2$ film may maintain tetragonal phase even at room temperature as long as the bi-axial strain in the (001)-VO$_2$ thin film does not relax with the film-thickness below the critical thickness (~26.5 nm) in the hetero-epitaxial system.

According to the above discussion, the structural phase transition and electronic transition appeared simultaneously in the thicker VO$_2$ films due to the relaxation of the strain. However, for the ultrathin strained VO$_2$ films, the structural phase transition can be suppressed by the interfacial epitaxial strain in the vicinity of the MIT temperature. We conjecture that the structural phase transition may be finished at much lower temperature due to the strain effect, which will be studied in the future research.

Conclusions

The (001)-VO$_2$ films with various thicknesses were fabricated via RF magnetron sputtering, and the structural and electronic transitions were studied by temperature-dependent XRD-RSM, Raman spectroscopy, and UPS. The XRD-RSM results show that there is no structural phase transition during MIT, and the Raman spectra further confirms that the ultrathin VO$_2$ film is tetragonal in both insulating and metallic states by epitaxial strain. The UPS confirmed that the MIT is induced solely by the electronic transition, which demonstrates that the MIT could be a pure Mott transition in the strained (001)-VO$_2$/TiO$_2$ epitaxial films. Furthermore, the absence of a structural phase transition is confirmed by DFT calculations. The electron-electron interactions should be the driving force for the MIT in the strained VO$_2$ film. Our systematic study not only provide a better understanding of the MIT mechanism for strained (001)-VO$_2$/TiO$_2$ thin films, but also show some clues to modulate the MIT via strain engineering. Furthermore, a series thickness of (001)-VO$_2$/TiO$_2$ around the critical thickness (~26.5 nm) should be prepared for further confirmation the strain-controlled behaviors of the MIT. Moreover, much more experimental and theoretical studies for the MIT mechanism of strained or relaxed VO$_2$ films on the other oriented TiO$_2$ ((011) or (111)) substrates are desired in future, which will be helpful to understand the MIT mechanism of the strained VO$_2$/TiO$_2$ thin films comprehensively.

Methods

Sample fabrication. The ultrathin VO$_2$/TiO$_2$ films were fabricated on (001)-oriented TiO$_2$ substrates purchased from Hefei Kejing Materials Technology Corporation using reactive radio frequency (RF) magnetron sputtering. A 99.99%-purity vanadium metal target was sputtered at 60 W RF power at a sputtering pressure of 0.43 Pa. The growth temperature was set to 400 °C and the Ar:O$_2$ flow ratio was 60:0.5[60].

X-ray diffraction characterization. To characterize the growth quality and structure of the VO$_2$ films, both conventional XRD scans and synchrotron radiation reciprocal space mapping (RSM) were performed. The XRD θ–2θ and φ scans were performed on a four-circle diffractometer with a Ge (220) × 2 incident-beam monochromator (Rigaku SmartLab Film Version, Cu-$K\alpha$ radiation). The RSMs were collected at beamline BL14B1 on the Shanghai Synchrotron Radiation Facility (SSRF, $\lambda = 0.124$ nm). The results were plotted in the reciprocal lattice units (r.l.u.) of TiO$_2$.

Raman spectroscopy. *In situ* temperature-controlled Raman spectroscopy with acquisition time of 20 s was acquired using the XploRA™ Raman spectrometer (HORIBA Scientific, Ltd). A 532 nm laser of 0.25 mW was used as the excitation source with a 100× microscope objective. To perform temperature-dependent measurements, a home-made, actively-controlled heating stage was equipped on the sample with an accuracy of 0.5 °C. Each Raman spectrum was acquired three times after the temperature was stable.

Ultraviolet Photoelectron Spectroscopy. Ultraviolet Photoelectron Spectroscopy (UPS) was used to study the V 3d electronic states near the Fermi energy E_F. These experiments were performed at the Catalysis and Surface Physics Endstation with the BL11U beamline on the National Synchrotron Radiation Laboratory (NSRL) in Hefei, China. The temperature-dependent valence-band spectra were measured with a VG Scienta R4000 analyzer with photon energy of 21.2 eV as the excitation source—this was calibrated with the Fermi level determined by the Au sample. In addition, the heating controller (temperature control range: 90–1400 K) offers a stable and precise temperature with 0.1 °C accuracy. Prior to UPS measurements, the films were subjected to argon ion sputtering to expose a clean surface of the film to UV light.

Theoretical calculations. The density functional theory (DFT) calculations were carried out with DFT+U where U is the Hubbard electron-electron correlation parameter. We used the Materials Studio calculation package equipped on Supercomputing Center of the University of Science and Technology of China. We adopted the Perdew-Burke-Ernzerhof functional under generalized gradient approximation (GGA) for the exchange correlation along with double-ζ-double polarized basis set for the electron wave function.

References

1. Morin, F. J. Oxides which show a metal-to-insulator transition at the Neel temperature. *Phys. Rev. Lett.* **3,** 34–36 (1959).
2. Liu, M. *et al.* Phase transition in bulk single crystals and thin films of VO$_2$ by nanoscale infrared spectroscopy and imaging. *Phys. Rev. B* **91,** 245155 (2015).
3. Nakajima, M., Takubo, N., Hiroi, Z., Ueda, Y. & Suemoto, T. Photoinduced metallic state in VO$_2$ proved by the terahertz pump-probe spectroscopy. *Appl. Phys. Lett.* **92,** 011907 (2008).
4. Mandal, P., Speck, A., Ko, C. & Ramanathan, S. Terahertz spectroscopy studies on epitaxial vanadium dioxide thin films across the metal-insulator transition. *Opt. Lett.* **36,** 1927–1929 (2011).
5. Sim, J. S., Zhou, Y. & Ramanathan, S. Suspended sub-50 nm vanadium dioxide membrane transistors: fabrication and ionic liquid gating studies. *Nanoscale* **4,** 7056–7062 (2012).
6. Driscoll, T. *et al.* Memory metamaterials. *Science* **325,** 1518–1521 (2009).
7. Wang, D. *et al.* Switchable ultrathin quarter-wave plate in terahertz using active phase-change metasurface. *Sci. Rep.* **5,** 15020 (2015).
8. Seo, M. *et al.* Active terahertz nanoantennas based on VO$_2$ phase transition. *Nano Lett.* **10,** 2064 (2010).

8

9. Zhou, J. *et al.* VO$_2$ thermochromic smart window for energy savings and generation. *Sci. Rep.* **3,** 3029 (2013).
10. Hu, C. *et al.* VO$_2$/TiO$_2$ nanosponges as binder-free electrodes for high-performance supercapacitors. *Sci. Rep.* **5,** 16012 (2015).
11. Wu, J. *et al.* Strain-induced self organization of metal-insulator domains in single-crystalline VO$_2$ nanobeams. *Nano Lett.* **6,** 2313–2317 (2006).
12. Kumar, S. *et al.* Sequential electronic and structural transitions in VO$_2$ observed using x-ray absorption spectromicroscopy. *Adv. Mater.* **26,** 7505–7509 (2014).
13. Hada, M., Okimura, K. & Matsuo, J. Characterization of structural dynamics of VO$_2$ thin film on *c*-Al$_2$O$_3$ using in-air time-resolved x-ray diffraction. *Phys. Rev. B* **82,** 153401 (2010).
14. Qazilbash, M. M. *et al.* Mott transition in VO$_2$ revealed by infrared spectroscopy and nano-imaging. *Science* **318,** 1750–1753 (2007).
15. Kim, H. T. *et al.* Mechanism and observation of Mott transition in VO$_2$-based two- and three- terminal devices. *New J. Phys.* **6,** 52 (2004).
16. Booth, J. M. & Casey, P. S. Anisotropic structure deformation in the VO$_2$ metal-insulator transition. *Phys. Rev. Lett.* **103,** 086402 (2009).
17. Kim, S., Kim, K., Kang, C. J. & Min, B. I. Correlation-assisted phonon softening and the orbital-selective Peierls transition in VO$_2$. *Phys. Rev. B* **87,** 195106 (2013).
18. Yao, T. *et al.* Understanding the nature of the kinetic process in a VO$_2$ metal-insulator transition. *Phys. Rev. Lett.* **105,** 226405 (2010).
19. Cocker, T. L. *et al.* Phase diagram of the ultrafast photoinduced insulator-metal transition in vanadium dioxide. *Phys. Rev. B* **85,** 155120 (2012).
20. Zylbersztejn, A. & Mott, N. F. Metal-insulator transition in vanadium dioxide. *Phys. Rev. B* **11,** 4383 (1975).
21. Kim, H. T. *et al.* Monoclinic and correlated metal phase in VO$_2$ as evidence of the Mott transition: coherent phonon analysis. *Phys. Rev. Lett.* **97,** 266401 (2006).
22. Tselev, A. *et al.* Symmetry relationship and strain-induced transitions between insulating M1 and M2 and metallic R phase of vanadium dioxide. *Nano Lett.* **10,** 4409–4416 (2010).
23. Morrison, V. R. *et al.* A photoinduced metal-like phase of monoclinic VO$_2$ revealed by ultrafast electron diffraction. *Science* **346,** 445 (2014).
24. Kim, B. J. *et al.* Micrometer x-ray diffraction study of VO$_2$ films: separation between metal-insulator transition and structural phase transition. *Phys. Rev. B* **77,** 235401 (2008).
25. Fan, L. L. *et al.* Strain dynamics of ultrathin VO$_2$ film grown on TiO$_2$ (001) and the associated phase transition modulation. *Nano Lett.* **14,** 4036–4043 (2014).
26. Kittiwatanakul, S., Wolf, S. A. & Lu, J. Large epitaxial bi-axial strain induced a Mott-like phase transition in VO$_2$. *Appl. Phys. Lett.* **105,** 261908 (2014).
27. Laverock, J. *et al.* Photoemission evidence for crossover from Peierls-like to Mott-like transition in highly strained VO$_2$. *Phys. Rev. B* **86,** 195124 (2012).
28. Yang, Y. J. *et al.* Anomalous thickness-dependent strain states and strain-tunable magnetization in Zn-doped ferrite epitaxial films. *J. Appl. Phys.* **115,** 173505 (2014).
29. Liu, L., Zhang, Y. & Zhang, T. Strain relaxation in heteroepitaxial films by misfit twinning. I. critical thickness. *J. Appl. Phys.* **101,** 063501 (2007).
30. Laverock, J. *et al.* Direct observation of decoupled structural and electronic transitions and an ambient pressure monocliniclike metallic phase of VO$_2$. *Phys. Rev. Lett.* **113,** 216402 (2014).
31. Matthews, J. W. & Blakeslee, A. E. Defects in epitaxial multilayers: I. misfit dislocations. *J. Cryst. Growth* **27,** 118 (1974).
32. Nagashima, K., Yanagida, T., Tanaka, H. & Kawai, T. Interface effect on metal-insulator transition of strained vanadium dioxide ultrathin films. *J. Appl. Phys.* **101,** 026103 (2007).
33. Yang, M. M. *et al.* Surface-growth-mode-induced strain effects on the metal-insulator transition in epitaxial vanadium dioxide thin films. *RSC Adv.* **5,** 80122 (2015).
34. Liu, M. K. *et al.* Anisotropic electronic state via spontaneous phase separation in strained vanadium dioxide films. *Phys. Rev. Lett.* **111,** 096602 (2013).
35. Muraoka, Y. & Hiroi, Z. Metal-insulator transition of VO$_2$ thin films grown on TiO$_2$ (001) and (110) substrates. *Appl. Phys. Lett.* **80,** 583 (2002).
36. Quackenbush, N. F. *et al.* Nature of the metal insulator transition in ultrathin epitaxial vanadium dioxide. *Nano Lett.* **13,** 4857–4861 (2013).
37. Jeong, J. *et al.* Suppression of metal-insulator transition in VO$_2$ by electric field-induced oxygen vacancy formation. *Science* **339,** 1402–1405 (2013).
38. Zhang, P. *et al.* Manipulations from oxygen partial pressure on the higher energy electronic transition and dielectric function of VO$_2$ films during a metal-insulator transition process. *J. Mater. Chem. C* **3,** 5033 (2015).
39. Ruzmetov, D., Senanayake, S. D., Narayanamurti, V. & Ramanathan, S. Correlation between metal-insulator transition characteristics and electronic structure changes in vanadium oxide thin films. *Phys. Rev. B* **77,** 195442 (2008).
40. Abreu, E. *et al.* THz spectroscopy of VO$_2$ epitaxial films: controlling the anisotropic properties through strain engineering. *New J. Phys.* **14,** 083026 (2012).
41. Radue, E. *et al.* Effect of a substrate-induced microstructure on the optical properties of the insulator-metal transition temperature in VO$_2$ thin films. *J. Appl. Phys.* **113,** 233104 (2013).
42. Chang, S. J. *et al.* *In situ* probing of doping- and stress-mediated phase transitions in a single-crystalline VO$_2$ nanobeam by spatially resolved Raman spectroscopy. *Nanoscale* **6,** 8068–8074 (2014).
43. Chen, X. B. Assignment of the Raman modes of VO$_2$ in the monoclinic insulating phase. *Journal of the Korean Physical Society* **58,** 100 (2011).
44. Schilbe, P. Raman scattering in VO$_2$. *Physica B* **316,** 600–602 (2002).
45. Sun, C., Yan, L., Yue, B., Liu, H. & Gao, Y. The modulation of metal-insulator transition temperature of vanadium dioxide: a density functional theory study. *J. Mater. Chem. C* **2,** 9283–9293 (2014).
46. Kim, H. T. *et al.* Raman study of electric-field-induced first-order metal-insulator transition in VO$_2$-based devices. *Appl. Phys. Lett.* **86,** 242101 (2005).
47. Saeki, K. *et al.* Band dispersion near the Fermi level for VO$_2$ thin films grown on TiO$_2$ (001) substrates. *Phys. Rev. B* **80,** 125406 (2009).
48. Koethe, T. C. *et al.* Transfer of spectral weight and symmetry across the metal-insulator transition in VO$_2$. *Phys. Rev. Lett.* **97,** 116402 (2006).
49. Eguchi, R. *et al.* Photoemission evidence for a Mott-Hubbard metal-insulator transition in VO$_2$. *Phys. Rev. B* **78,** 075115 (2008).
50. Okazaki, K. *et al.* Photoemission study of the metal-insulator transition in VO$_2$/TiO$_2$(001): evidence for strong electron-electron and electron-phonon interaction. *Phys. Rev. B* **69,** 165104 (2004).
51. Okimura, K. *et al.* Temperature-dependent Raman and ultraviolet photoelectron spectroscopy studies on phase transition behavior of VO$_2$ films with M1 and M2 phases. *J. Appl. Phys.* **115,** 153501 (2014).
52. Karel, J. *et al.* Distinct electronic structure of the electrolyte gate-induced conducting phase in vanadium dioxide revealed by high-energy photoelectron spectroscopy. *ACS Nano* **8,** 5784–5789 (2014).
53. Goodenough, J. B. The two components of the crystallographic transition in VO$_2$. *J. Solid State. Chem.* **3,** 490–500 (1971).

54. Aetukuri, N. B. *et al.* Control of the metal-insulator transition in vanadium dioxide by modifying orbital occupancy. *Nat. Phys.* **9,** 661–666 (2013).

55. Huefner, M. *et al.* Hubbard gap modulation in vanadium dioxide nanoscale tunnel junctions. *Nano Lett.* **14,** 6115–6120 (2014).

56. Wu, Y. *et al.* Decoupling the lattice distortion and charge doping effects on the phase transition behaviourof VO_2 by titanium (Ti^{4+}) doping. *Sci. Rep.* **5,** 9328 (2015).

57. Wegkamp, D. *et al.* Instantaneous band gap collapse in photoexcited monoclinic VO_2 due to photocarrier doping. *Phys. Rev. Lett.* **113,** 216401 (2014).

58. Lazarovits, B., Kim, K., Haule, K. & Kotliar, G. Effects of strain on the electronic structure of VO_2. *Phys. Rev. B* **81,** 115117 (2010).

59. Weber, C. *et al.* Vanadium dioxide: a Peierls-Mott insulator stable against disorder. *Phys. Rev. Lett.* **108,** 256402 (2012).

60. Yang, M. M. *et al.* Resistance switching of epitaxial VO_2/Al_2O_3 heterostructure at room temperature induced by organic liquids. *AIP Adv*. **5,** 037114 (2015).

Acknowledgements

Author Contributions

Both authors, M.Y. and Y.Y. contributed equally to the research and to the preparation of the manuscript. Y.Y. conceived this work. C.G. and Z.L. designed the whole study. M.Y. and L.W. fabricated the samples. M.Y. and Y.Y. performed all the experiments. M.Y. wrote the paper. B.H., Y.Y. and M.Y. performed the DFT calculations. K.H., J.Z. and H.H. performed normal XRD studies. H.C. and L.S. measured the Raman spectra. J.B. and X.L. analyzed the data and discussed the results and reviewed the manuscript. Y.D., Y.G., T.Y. and X.G. performed *in situ* temperature-dependent high-resolution XRD on synchrotron radiation. H.X. analyzed the XRD results and prepared the figures. H.J. and J.Z. performed the XPS experiments and analyzed the XPS data. All authors reviewed and revised the manuscript.

Additional Information

Supplementary information accompanies this paper at http://www.nature.com/srep

Competing financial interests: The authors declare no competing financial interests.

How to cite this article: Yang, M. *et al.* Suppression of Structural Phase Transition in VO_2 by Epitaxial Strain in Vicinity of Metal-insulator Transition. *Sci. Rep.* **6**, 23119; doi: 10.1038/srep23119 (2016).